

A new parton model for the soft interactions at high energies: two channel approximation.

E. Gotsman,^{1,*} E. Levin,^{1,2,†} and I. Potashnikova^{2,‡}

¹*Department of Particle Physics, School of Physics and Astronomy,
Raymond and Beverly Sackler Faculty of Exact Science, Tel Aviv University, Tel Aviv, 69978, Israel*

²*Departemento de Física, Universidad Técnica Federico Santa María, and Centro Científico-Tecnológico de Valparaíso, Avda. Espana 1680, Casilla 110-V, Valparaíso, Chile*

(Dated: September 11, 2022)

In this paper we manage to achieve a fairly good description of four experimental observables: $\sigma_{\text{tot}}, \sigma_{\text{el}}, B_{\text{el}}$ and the single diffraction cross sections, for proton-proton scattering, in a two channel model for the structure of hadrons at high energy. The impact parameter dependence of the scattering amplitudes show that soft interactions at high energies measured at the LHC, have a much richer structure than presumed. We discuss the t -dependence of the elastic cross section in wide range of $|t| = 0 \div 1 \text{ GeV}^2$.

Our approach has been discussed in a recent paper [1] and it is based (i) on Pomeron calculus in 1+1 space-time, suggested in Ref. [2], and (ii) on simple assumptions of hadron structure, related to the impact parameter dependence of the scattering amplitude. This parton model stems from QCD, assuming that the unknown non-perturbative corrections lead to determining the size of the interacting dipoles. The advantage of this approach is that it satisfies both the t -channel and s -channel unitarity, and can be used for summing all diagrams of the Pomeron interaction, including Pomeron loops. In other words, we can use this approach for all possible reactions: dilute-dilute (hadron-hadron), dilute-dense (hadron-nucleus) and dense-dense (nucleus-nucleus), parton systems scattering. Hence, we present in the paper the first description of the data (for proton-proton scattering) based on a model that satisfies both t and s channel unitarity.

PACS numbers: 12.38.-t, 24.85.+p, 25.75.-q

Contents

Introduction	1
The new parton model	2
General approach.	2
Interrelation with QCD.	3
Two channel approximation	3
The general formulae.	3
Physical observables.	5
Comparison with experimental data for proton-proton scattering	5
Dependence on impact parameters	6
Dependence of the elastic cross sections on t	7
Conclusions	10
References	12

INTRODUCTION

In our recent paper [1] we proposed a new parton model for high energy soft interactions, which is based on Pomeron calculus in 1+1 space-time dimensions, suggested in Ref. [2], and on simple assumptions of hadron structure, related to the impact parameter dependence of the scattering amplitude. This parton model stems from QCD, assuming that the unknown non-perturbative corrections lead to determining the size of the interacting dipoles. The advantage of this approach is that it satisfies both the t -channel and s -channel unitarity, and can be used for summing all

diagrams of the Pomeron interaction including Pomeron loops. In other words, we can use this approach for all possible reactions: dilute-dilute (hadron-hadron), dilute-dense (hadron-nucleus) and dense-dense (nucleus-nucleus) parton system scattering.

We showed that this model is able to describe high energy data on the total and elastic cross sections for proton-proton scattering, but the simple version of Ref.[1] leads to vanishing of diffractive production. In this paper we propose a two channel model which generates diffraction production in the region of small masses. We demonstrate that a two channel model is able to describe four experimental observables: $\sigma_{\text{tot}}, \sigma_{\text{el}}, B_{\text{el}}$ and the single diffraction cross sections. We show that this model leads to a rich structure for the impact parameter dependence of the scattering amplitude. In particular, we study the dependence of the elastic cross section as function of $|t| = 0 \div 1 \text{ GeV}^2$. It is shown that we are able to describe the experimental data on $d\sigma_{\text{el}}/dt$ in this t -region: the position of the minimum with $|t|_{\text{min}} = 0.52 \text{ GeV}^2$ at $W = 7 \text{ TeV}$ and the value and t behaviour for larger t .

THE NEW PARTON MODEL

General approach.

As we have discussed in Ref.[1, 2] the new parton model is based on three ingredients:

1. The Colour Glass Condensate (GCC) approach (see Ref.[3] for a review), which can be re-written in the equivalent form as the interaction of BFKL Pomerons[4] in a limited range of rapidities ($Y \leq Y_{\text{max}}$):

$$Y \leq \frac{2}{\Delta_{\text{BFKL}}} \ln \left(\frac{1}{\Delta_{\text{BFKL}}^2} \right) \quad (1)$$

Δ_{BFKL} denotes the intercept of the BFKL Pomeron[5]. In our model $\Delta_{\text{BFKL}} \approx 0.2 - 0.25$ leading to $Y_{\text{max}} = 20 - 30$, which covers all collider energies.

2. The following Hamiltonian:

$$\mathcal{H}_{\text{NPM}} = -\frac{1}{\gamma} \bar{P} P \quad (2)$$

where NPM stands for ‘‘new parton model’’. P and \bar{P} are the BFKL Pomeron fields. The fact that it is self dual is evident. This Hamiltonian in the limit of small \bar{P} reproduces the Balitsky-Kovchegov Hamiltonian \mathcal{H}_{BK} (see Ref.[2] for details). This condition is the most important one for determining the form of \mathcal{H}_{NPM} . γ in Eq. (2) denotes the dipole-dipole scattering amplitude, which in QCD is proportional to $\bar{\alpha}_S^2$.

3. The new commutation relations:

$$(1 - P)(1 - \bar{P}) = (1 - \gamma)(1 - \bar{P})(1 - P) \quad (3)$$

For small γ and in the regime where P and \bar{P} are also small, we obtain

$$[P, \bar{P}] = -\gamma + \dots \quad (4)$$

consistent with the standard BFKL Pomeron calculus (see Ref.[2] for details) .

In Ref.[2], it was proved that the scattering matrix for the model is given by

$$\begin{aligned} S_{m\bar{n}}^{\text{NPM}}(Y) &= e^{\frac{1}{\gamma} \int_0^Y d\eta [\ln(1-p) \frac{\partial}{\partial \eta} \ln(1-\bar{p}) + \bar{p}p]} [1 - p(Y)]^m [1 - \bar{p}(0)]^{\bar{n}} \Big|_{p(0)=1-e^{-\gamma\bar{n}}; \bar{p}(Y)=1-e^{-\gamma m}} \\ &= [1 - p(Y)]^m e^{\frac{1}{\gamma} \int_0^Y d\eta [\ln(1-\bar{p}) + \bar{p}]} \end{aligned} \quad (5)$$

where $p(\eta)$ and $\bar{p}(\eta)$ are solutions of the classical equations of motion and have the form:

$$P(\eta) = \frac{\alpha + \beta e^{(1-\alpha)\eta}}{1 + \beta e^{(1-\alpha)\eta}}; \quad \bar{P}(\eta) = \frac{\alpha(1 + \beta e^{(1-\alpha)\eta})}{\alpha + \beta e^{(1-\alpha)\eta}}; \quad (6)$$

where the parameters β and α should be determined from the boundary conditions:

$$P(\eta = 0) = p_0; \quad \bar{P}(\eta = Y) = \frac{\alpha}{P(\eta = Y)} = \bar{p}_0 \quad (7)$$

It is interesting to compare the scattering amplitude given by this expression to that obtained from the BK equation, which describes deep inelastic scattering on nuclei in QCD. For which we have

$$S_{m\bar{n}}^{\text{BK}}(Y) = \int dP(\eta)d\bar{P}(\eta)e^{\frac{1}{\gamma} \int_0^Y d\eta [\ln(1-P)\frac{\partial}{\partial\eta} \ln(1-\bar{P}) - \ln(1-\bar{P})PP]} (1-P(Y))^m (1-\bar{P}(0))^{\bar{n}} \quad (8)$$

In the classical approximation

$$\begin{aligned} S_{m\bar{n}}^{\text{BK}}(Y) &= e^{\frac{1}{\gamma} \int_0^Y d\eta [\ln(1-p)\frac{\partial}{\partial\eta} \ln(1-\bar{p}) - \ln(1-\bar{p})p]} [1-p(Y)]^m [1-\bar{p}(0)]^{\bar{n}} \Big|_{p(0)=1-e^{-\gamma\bar{n}}; \bar{p}(Y)=1-e^{-\gamma m}} \\ &= [1-p(Y)]^m \end{aligned} \quad (9)$$

Note, that the solution for \bar{P} , is not relevant for the BK amplitude, which is determined entirely by $P(Y)$. On the other hand the scattering amplitude in the NPM depends on \bar{P} . Nevertheless, the two models should be similar in the regime where the BK evolution is valid. The results of the estimates in Ref.[2] shows that in the region close to saturation, the differences between BK and NPM are quite significant.

Interrelation with QCD.

As has been mentioned, in the limited range of energies, given by Eq. (1), both QCD and our model describe the interaction of the BFKL Pomeron[5]. For weak fields P and \bar{P} , the model reproduces the BK limit of the CGC approach, assuming that the non-perturbative corrections result in determining the size of the interacting dipoles, and hence, the successful description of the soft data at high energies in CGC approach [6–13] supports the idea that this effective size is rather small. The model leads to the descriptions that satisfy both t -unitarity and s -channel unitarity, while, as it was shown in Ref.[2], the BFKL Pomeron calculus in the BK limit, as well as the Braun Hamiltonian[14] for dense-dense system scattering violates s -channel unitarity. Unfortunately, we are still far from being able to solve this problem in the effective QCD theory at high energy (i.e. in the CGC /saturation approach).

Two channel approximation

Our model includes three essential ingredients: (i) the new parton model for the dipole-dipole scattering amplitude that has been discussed above; (ii) the simplified two channel model that enables us to take into account diffractive production in the low mass region, and (iii) the assumptions for impact parameter dependence of the initial conditions.

In the two channel approximation we replace the rich structure of the diffractively produced states, by a single state with the wave function ψ_D . The observed physical hadronic and diffractive states are written in the form

$$\psi_h = \alpha \Psi_1 + \beta \Psi_2; \quad \psi_D = -\beta \Psi_1 + \alpha \Psi_2; \quad \text{where} \quad \alpha^2 + \beta^2 = 1; \quad (10)$$

Functions ψ_1 and ψ_2 form a complete set of orthogonal functions $\{\psi_i\}$ which diagonalize the interaction matrix \mathbf{T}

$$A_{i,k}^{i'k'} = \langle \psi_i \psi_k | \mathbf{T} | \psi_{i'} \psi_{k'} \rangle = A_{i,k} \delta_{i,i'} \delta_{k,k'}. \quad (11)$$

The unitarity constraints take the form

$$2 \text{Im} A_{i,k}(s, b) = |A_{i,k}(s, b)|^2 + G_{i,k}^{in}(s, b), \quad (12)$$

where $G_{i,k}^{in}$ denotes the contribution of all non diffractive inelastic processes, i.e. it is the summed probability for these final states to be produced in the scattering of a state i off a state k . In Eq. (12) $\sqrt{s} = W$ denotes the energy of the colliding hadrons and b denotes the impact parameter. In our approach we used the solution to Eq. (12) given by Eq. (5) and

$$A_{ik} = 1 - S_{ik}^{\text{NPM}}(Y) \quad (13)$$

The general formulae.

Initial conditions: Following Ref.[1] we chose the initial conditions in the form:

$$p_i(b') = p_{0i} S(b', m_i) \quad \text{with} \quad S(b, m_i) = m_i b K_1(m_i b); \quad \bar{p}_i(\mathbf{b} - \mathbf{b}') = p_{0i} S(\mathbf{b} - \mathbf{b}', m_i) \quad z_m = e^{\Delta(1-p_{01})Y} \quad (14)$$

Both p_{0i} and masses m_i , as well as the Pomeron intercept Δ , are parameters of the model, which are determined by fitting to the relevant data. Note, that $S(b, m_i) \xrightarrow{m_i b \gg 1} \exp(-m_i b)$ in accord with the Froissart theorem[15],

From Eq. (14) we find that

$$a_{ik}(b, b') \equiv a_{i,k}(p_i, \bar{p}_k, z_m) = \frac{1}{2}(p_i + \bar{p}_k) + \frac{1}{2z_m}((1-p_i)(1-\bar{p}_k) - D_{i,k}); \quad (15)$$

$$b_{i,k}(b, b') \equiv b_{i,k}(p_i, \bar{p}_k, z_m) = \frac{1}{2} \frac{p_i - \bar{p}_k}{1-p_i} - \frac{1}{2z_m(1-p_i)}((1-p_i)(1-\bar{p}_k) - D_{i,k}); \quad (16)$$

$$D_{i,k} = \sqrt{4p_i(1-p_i)(1-\bar{p}_k)z_m - ((1-p_i)(1-\bar{p}_k) - (p_i - \bar{p}_k)z_m)^2}; \quad (17)$$

These equation are the explicit solutions to Eq. (6) and Eq. (7).

Amplitudes: In the following equations $p_i \equiv p_i(b')$ and $\bar{p}_k \equiv \bar{p}_k(\mathbf{b} - \mathbf{b}')$.

$$z = e^{\Delta(1-p_{01})y}$$

$$S_{ik}(a_{ik}, b_{ik}, z) \equiv S(a_{ik}(b, b'), b_{ik}(b, b'), z_m), \quad X_{i,k}(a, b, z) \equiv X(a_{ik}(b, b'), b_{ik}(b, b'), z_m)$$

$$X(a_{ik}, b_{ik}, z) = \frac{a_{ik} + b_{ik}z}{1 + b_{ik}z} \quad (18)$$

$$SS_{ik}(a_{ik}, b_{ik}, z) = \quad (19)$$

$$\begin{aligned} & -(a_{ik} - 1)\text{Li}_2(-b_{ik}z) + a_{ik}\text{Li}_2\left(-\frac{b_{ik}z}{a_{ik}}\right) + (a_{ik} - 1)\text{Li}_2\left(\frac{a_{ik} + b_{ik}z}{a_{ik} - 1}\right) + \frac{1}{2}a_{ik}\log^2((1 - a_{ik})b_{ik}z) \\ & -(a_{ik} - 1)\log(b_{ik}z + 1)\log((1 - a_{ik})b_{ik}z) - \left(a_{ik}\log(z) - (a_{ik} - 1)\log\left(-\frac{b_{ik}z + 1}{a_{ik} - 1}\right)\right)\log(a_{ik} + b_{ik}z) \\ & + a_{ik}\log(z)\log\left(\frac{b_{ik}z}{a_{ik}} + 1\right) \end{aligned}$$

$$S_{ik}(a_{ik}, b_{ik}, z) = SS_{ik}(a_{ik}, b_{ik}, z) - SS_{ik}(a_{ik}, b_{ik}, z = 1) \quad (20)$$

The amplitude is given by

$$\begin{aligned} A_{ik}(s, b) = & \quad (21) \\ 1 - \exp\left(\frac{1}{p_{01}} \int \frac{m_1^2 d^2 b'}{4\pi} \left(S_{ik}(a_{ik}, b_{ik}, z_m) + a_{ik}(b, b')\Delta(1-p_0)Y \right) - \int \frac{m_1^2 d^2 b'}{4\pi} \bar{p}_k(\mathbf{b} - \mathbf{b}', m_k) X(a_{ik}, b_{ik}, z_m) \right) \end{aligned}$$

Physical observables.

The physical observables in this model can be written as follows

$$\text{elastic amplitude : } a_{el}(s, b) = i(\alpha^4 A_{1,1} + 2\alpha^2 \beta^2 A_{1,2} + \beta^4 A_{2,2}); \quad (22)$$

$$\text{elastic cross section : } \sigma_{tot} = 2 \int d^2b a_{el}(s, b); \quad \sigma_{el} = \int d^2b |a_{el}(s, b)|^2;$$

$$\text{elastic slope : } B_{el} = \frac{1}{2} \frac{\int b^2 d^2b \text{Im}A_{el}(Y, b)}{\int d^2b \text{Im}A_{el}(Y, b)}; \quad (23)$$

$$\text{optical theorem : } 2 \text{Im}A_{el}(s, t=0) = 2 \int d^2b \text{Im}a_{el}(s, b) = \sigma_{el} + \sigma_{in} = \sigma_{tot}; \quad (24)$$

$$\text{elastic cross section : } \frac{d\sigma_{el}}{dt} = \pi |f(s, t)|^2; \quad a_{el}(s, b) = \frac{1}{2\pi} \int d^2q e^{-i\mathbf{q}\cdot\mathbf{b}} f(s, t) \text{ where } t = -q^2; \quad (25)$$

$$\text{single diffraction : } \sigma_{sd}^{GW} = 2 \int d^2b (\alpha\beta \{-\alpha^2 A_{1,1} + (\alpha^2 - \beta^2)A_{1,2} + \beta^2 A_{2,2}\})^2; \quad (26)$$

$$\text{double diffraction : } \sigma_{dd}^{GW} = \int d^2b \alpha^4 \beta^4 \{A_{1,1} - 2A_{1,2} + A_{2,2}\}^2. \quad (27)$$

It should be noted that factor 2 in Eq. (26) takes into account the single diffractive dissociation of the two protons.

COMPARISON WITH EXPERIMENTAL DATA FOR PROTON-PROTON SCATTERING

As we have seen in the previous section, we introduce three dimensionless parameters: Δ - the intercept of the BFKL Pomeron, and p_{01} (p_{02}) - the amplitudes of the dipole-dipole scattering at low energies, and β which is related to the contribution of the diffractive production. For b -dependence we suggested a specific form (see Eq. (14)) which is characterized by the dimensional parameters: m_i . These parameters are determined by fitting to the experimental data. We choose to describe five observables: total and elastic cross sections, the elastic slope and single and double diffractions at low masses (see Eq. (22)-Eq. (27)).

The situation with the experimental data on the single and double diffraction production in proton-proton scattering at high energies, is far from clear. It was well summarized in Ref.[19], to which we refer the reader. We assume that the two channel model is able to describe proton-proton diffraction production in the entire kinematic region of produced mass. As is shown in Ref.[21] for $\Delta > 0$ the integral over the produced mass in diffraction is convergent, and the Good-Walker mechanism[20] is able to describe the diffraction production both of small and large masses. However, the simple two channel model is a simplification, but we hope to learn something by attempting to fit all available data using this simple model.

From Fig. 1 one can see that we can describe the data for $W \geq 0.5 TeV$. The values of parameters of the fit are shown in Table I. The two sets of parameters have quite different values of m_1 and m_2 . However, note that the set of parameters I in Table I does not describe σ_{el} well, having the better value of $\chi^2/d.o.f$. This fact means that the set I produces a better fit to the diffractive data.

Comparing these parameters with the resulting curves in Fig. 1 we see that the shadowing corrections play an essential role. First, we note that the value of $\Delta_{dressed} = \Delta(1 - p_{01})$ is rather large (about 0.5) in all variants. Recall, that means that $\Delta \approx 1$. Factor $(1 - p_{01})$ in $\Delta_{dressed}$, stems from the enhanced diagrams that contribute to the Green function of the Pomeron. The resulting $\sigma_{tot} \propto s^{\Delta_{eff}}$ with $\Delta_{eff} \approx 0.07$. Such a reduction from $\Delta_{dressed}$ to Δ_{eff} occurs due to the strong shadowing corrections.

As one can see from Fig. 2-a we describe the single diffraction production data, which has been taken from Ref.[22] and they are shown in Fig. 2-b. The TOTEM value of the single diffraction cross section is 9.1 ± 2.9 (see Ref.[22]), while our estimates lead to $\sigma_{sd}^{smd} = 12 - 13 mb$. As can be seen from Fig. 2-a and Fig. 2-b, our model leads to values of the single diffraction cross section, which are close to our predictions from the CGC motivated model of Ref.[9] (the curve GLM in Fig. 2-b). We refer the reader to Ref.[19] in which the situation with tensions between different experimental groups on the single diffraction cross section, has been discussed.

One can see from the Table II and from Fig. 3-a, that we are able to account for only half of the double diffractive cross section. This reflects the situation which we had in our previous attempts to describe this process[9]. As one can see from the Table II and Fig. 3-a we reproduce the energy behaviour of the experimental data on the double diffraction but cannot obtain the large value of the cross section at $W = 0.5 TeV$. The same problem is faced by the

other groups (see, for example, Ref.[19] and reference therein). In Fig. 3-a we plot our prediction to which we add the constant cross section to fit data at $W = 0.5 \text{ TeV}$. Adding this parameter, we describe the data. Concluding, we think that a good description of the double diffraction data will be achieved in future by developing a more complicated model for the hadron structure and accumulating more and better experimental data.

Variant of the fit	Δ_{dressed}	p_{01}	p_{02}	m_1 (GeV)	m_2 (GeV)	β^2	$\chi^2/\text{d.o.f}$
I	0.48 ± 0.01	0.72 ± 0.05	0.006 ± 0.001	1.033 ± 0.01	0.50 ± 0.09	0.25 ± 0.01	1.1
II	0.52 ± 0.01	0.644 ± 0.02	0.10 ± 0.01	1.04 ± 0.01	1.79 ± 0.02	0.32 ± 0.01	1.1

TABLE I: Fitted parameters. $\Delta_{\text{dressed}} = \Delta (1 - p_{01})$.

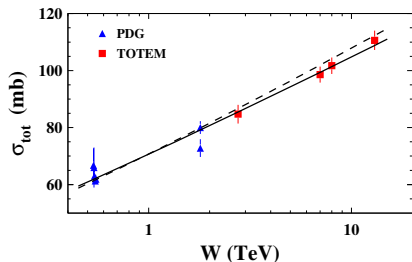


Fig. 1-a

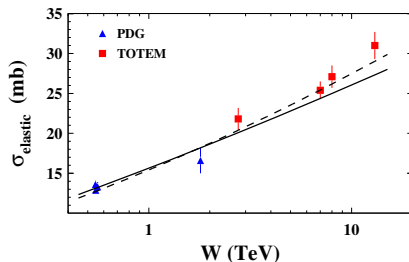


Fig. 1-b

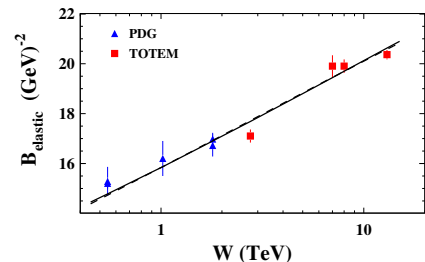


Fig. 1-c

FIG. 1: The energy behaviour of σ_{tot} , σ_{el} and the slope B_{el} for proton-proton scattering in our model. The solid line describes the variant I in Table I while the dashed line corresponds to variant II. Data are taken from Refs.[17, 18].

DEPENDENCE ON IMPACT PARAMETERS

In Fig. 4 we plot the scattering amplitudes as a function of the impact parameter b . One can see that the two channel model generates very interesting and unexpected structure. One amplitude $A_{11}(b)$ has reached the unitary limit $A_{11}(b=0) = 1$ at $W = 0.5 \text{ TeV}$ and shows the increasing of the radius of the interaction with energy. The two other amplitudes are far from the unitarity limit even at ultra high energy $W = 99 \text{ TeV}$. They increase as $W^{\Delta_{\text{eff}}}$ with $\Delta_{\text{eff}} \sim 0.1$. The behaviour as a function of b is also unexpected. Both A_{11} and A_{22} decrease monotonically at large b , while A_{12} has a maximum which moves to larger values of b , and the value of the amplitude for this maximum increases as $W^{\Delta_{\text{eff}}}$. On the other hand, $A_{12}(b=0)$ is almost independent on W .

Such dependence of the amplitudes generate the elastic amplitude which is smaller than the unitarity limit even at very high energies (see Fig. 4-a). This conclusion is in accord with the recent paper of Ref.[24] in which it is demonstrated that in the Miettinen-Pumplin [25] approach the elastic amplitude $A_{el}(b=0) \approx 0.92 < 1$ at $W = 57 \text{ TeV}$. Note, that this approach is ideologically close to ours and second, that in Ref.[24] the entire set of soft interaction data has been described successfully.

W (TeV)	σ_{tot} (mb)	σ_{el} (mb)	B_{el} (GeV^{-2})	σ_{sd} (mb)	σ_{dd} (mb)
0.55	61.86(61.59)	13.1(12.64)	14.78(14.80)	6.99(7.4)	1.1(1.41)
1.8	79.16(80.271)	18.178(18.14)	15.872(16.95)	9.55(10.14)	1.47(1.82)
2.76	85.4(87.08)	20.082(20.29)	17.686(17.73)	10.476(11.12)	1.63(1.95)
7	99.37(102.29)	24.37(25.32)	19.44(19.39)	12.464(13,14)	1.98(2.16)
8	101.4(104.5)	25.0(26.07)	19.695(19.62)	12.744 (13.4)	2.03(2.19)
13	108.811(112.61)	27.3(28.90)	20.623(20.46)	13.743 (14.40)	2.12(2.36)

TABLE II: The values of observables in our model for the set of parameters I. In parenthesis the values for the set II.

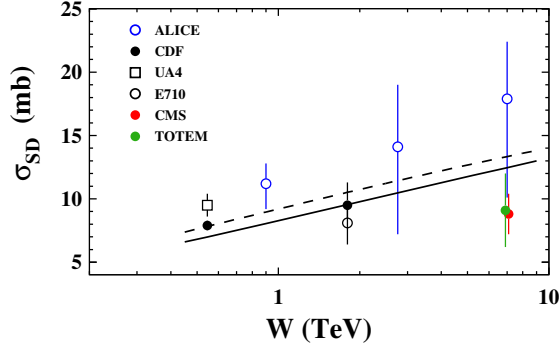


Fig. 2-a

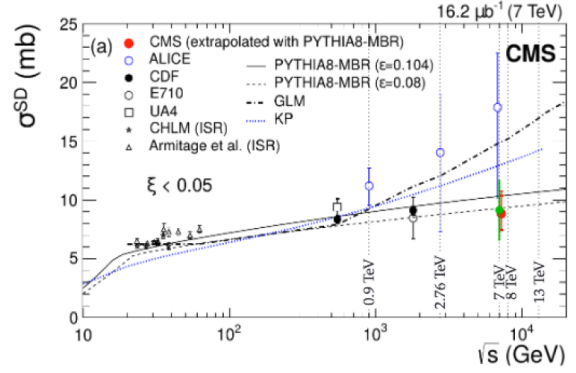


Fig. 2-b

FIG. 2: The single diffraction cross section as function of energy $W = \sqrt{s}$: our description of the data with $W \geq 0.5 \text{ TeV}$ (Fig. 2-a) and the experimental data from Ref.[22] (Fig. 2-b). The data of all experimental groups were extrapolated to the region $M^2 \leq 0.05 s$ using the Pythia Monte-Carlo programs as is shown in Fig. 2-b. M is the mass of hadron produced in single diffraction. The data in Fig. 2-a are taken from Ref.[22] and we refer to this paper (especially to Ref.[9] in it). The curves in Fig. 2-b marked as GLM are taken from Ref.[9] and that as KP is from Ref.[23].

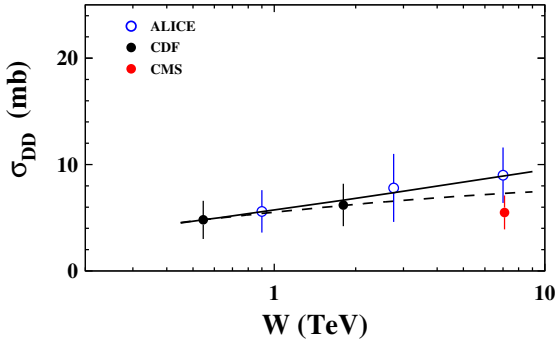


Fig. 3-a

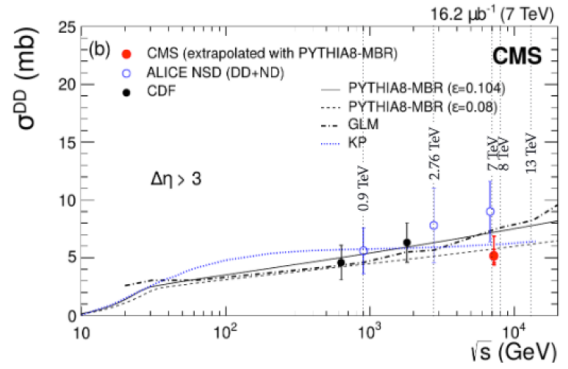


Fig. 3-b

FIG. 3: The double diffraction cross section as function of energy $W = \sqrt{s}$: our description (see text), solid and dashed lines correspond sets I and II of Table I (Fig. 3-a) the experimental points, were taken from Ref.[22].

In Fig. 2-a we present the comparison between the elastic amplitude in our 2 channel model and in one channel model of Ref. [1]. One can see that these two amplitudes have a different behaviour as a function of energy and impact parameter. We believe that this figure demonstrates that the modeling of the non-perturbative structure of the hadron is very important in understanding high energy scattering. Fig. 5-b shows the behaviour of $d\sigma_{sd}/db^2$ (see Eq. (26))

$$\frac{d\sigma_{sd}}{db^2} = (\alpha\beta\{-\alpha^2 A_{1,1} + (\alpha^2 - \beta^2)A_{1,2} + \beta^2 A_{2,2}\})^2 \quad (28)$$

One can see that this observable decreases very slowly with energy, and does not show a maximum at large b . Such behaviour is quite different from what we obtain in CGC motivated model (see Ref.[9] Fig.7) and from the estimates of Ref.[24].

Bearing in mind that we describe the experimental data fairly well, we believe that the impact parameter and energy behaviours shown in Fig. 4 and in Fig. 2, illustrate the fact that the soft interaction at high energies could have a much richer structure than we previously assumed.

DEPENDENCE OF THE ELASTIC CROSS SECTIONS ON t

We attempt to describe the elastic cross section for $|t| = 0 \div 1 \text{ GeV}^2$ to check the rich structure present in the

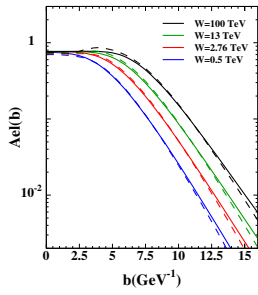


Fig. 4-a

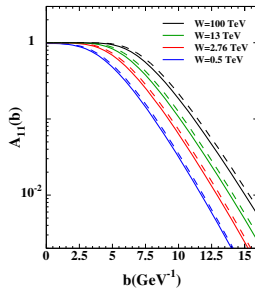


Fig. 4-b

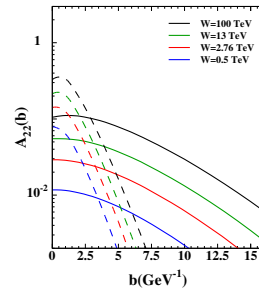


Fig. 4-c

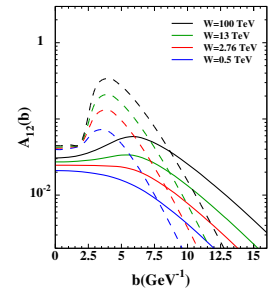


Fig. 4-d

FIG. 4: The scattering amplitudes versus impact parameter b for different energies: Fig. 4-a A_{el} ; Fig. 4-b A_{11} , Fig. 4-c A_{22} , Fig. 4-d A_{12} .

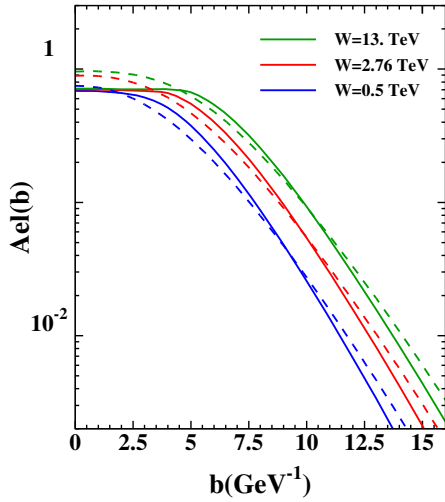


Fig. 5-a

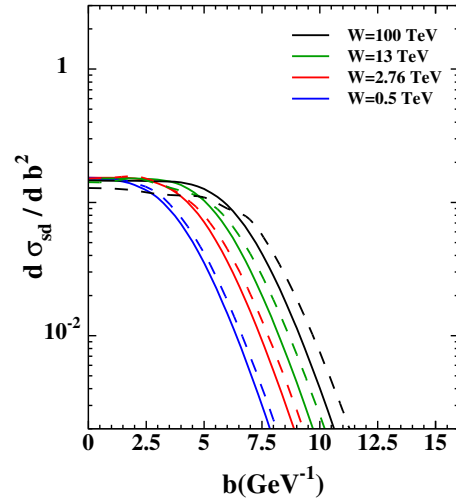


Fig. 5-b

FIG. 5: The scattering amplitudes versus impact parameter b for different energies: Fig. 5-a: the elastic amplitudes for the one channel model of Ref.[1] (dashed line) and for two channel model of this paper (solid line). For estimates in our model we used set I of parameters in Table I; Fig. 5-b: $\frac{d\sigma_{sd}}{db^2}$ of Eq. (28) for the variant two (solid line) and variant one (dashed line) set of parameters.

impact parameter dependence, this stems from our model, which predicts the existence of a minimum in the elastic cross sections, however its position occurs at $|t| \approx 0.3 GeV^2$, which is much smaller than was observed experimentally by TOTEM collaboration[26].

Assuming that this discrepancy has its roots due to the simplified form of b dependence of our amplitude which is given by Eq. (14), we changed the initial conditions of Eq. (14) to the following equations

$$p_i(b') = p_{0i} S(b', m_i, \mu_i, \kappa_i) \quad \text{with} \quad S(b, m_i, \mu_i, \kappa_i) = (1 - \kappa_i) (m_i b)^{\nu_1} K_{\nu_1}(m_i b) + \kappa_i \frac{(m_i b)^{\nu_2} K_{\nu_2}(\mu_i b)}{2^{\nu_2 - 1} \Gamma(\nu_2)} \quad (29)$$

For simplicity we made a fit using the one channel model in which $p_{01} \neq 0$ but $p_{02} = 0$. In the Table III we present the parameters that we found for the fit. Fig. 6 shows the comparison with TOTEM data of Ref.[26]. One can see that we have good agreement with the experimental data for $|t| < |t|_{min}$ and for $|t| > |t|_{min}$. However, for $|t| \approx |t|_{min}$ the real part of the scattering amplitude turns out to be small, and we obtain a value of the $d\sigma_{el}/dt$ approximately an order of magnitude smaller than the experimental one. It should be stressed that we do not use any of the simplified approaches to estimate the real part of the amplitude, but using our general expression of Eq. (21) for $A_{ik}(s, t)$, we consider the sum $A_{ik}(s, +i\epsilon t) + A_{ik}(u - i\epsilon, t)$, which corresponds to positive signature, and calculated the real part of this sum.

In Fig. 6 we estimate the contribution of the ω -reggeon, using the description taken from the paper of Ref.[27](note

the difference between green dashed line and the blue solid curve). This contribution is small, and can be neglected.

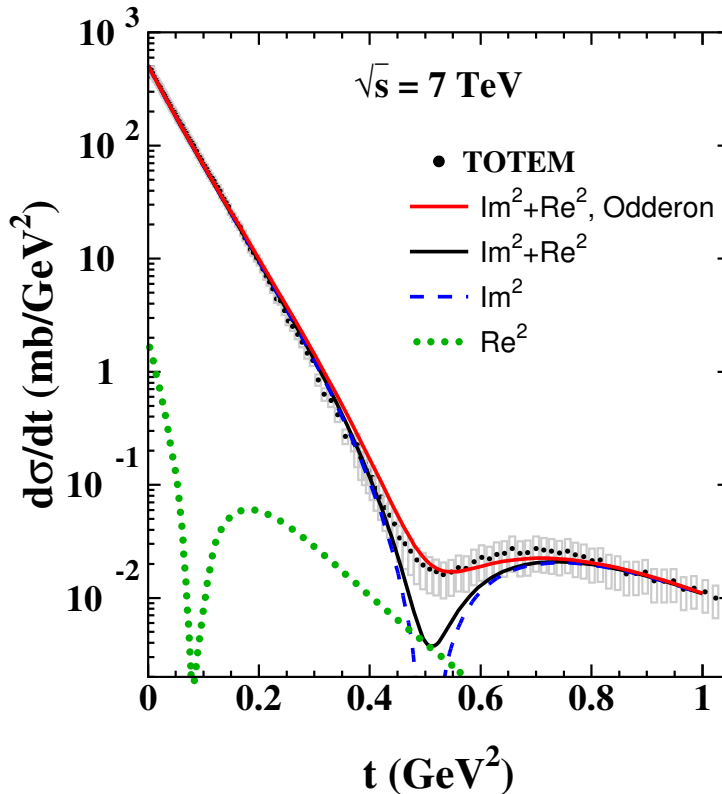


FIG. 6: $d\sigma_{el}/dt$ versus t . The black green line describes the result of our fit. The dashed line corresponds to the contribution of the imaginary part of the scattering amplitude to the elastic cross section. The dotted line relates to the real part of our amplitude. The red solid line takes into account the contribution of the odderon to the real part of the pp amplitude, as is shown in Eq. (32). The data, shown in grey, include systematic errors. They are taken from Ref.[26].

To evaluate the real part of the amplitude we use the relation:However,

$$\text{Re}A_{11}(s, t) = \frac{1}{2} \pi \frac{\partial}{\partial \ln(s/s_0)} \text{Im}A_{11}(s, t)|_{Eq. (21)} \quad (30)$$

Eq. (30) correctly describes the real part of the amplitude only for small $\rho = \text{Re}A/\text{Im}A$. In Fig. 7 we plot the $d\sigma/dt$ with such estimates for the real part. The real part from Eq. (30) turns out to be almost twice larger than the experimental data in the vicinity of t_{min} . Therefore, at the minimum, where $\text{Im}A \ll \text{Re}A$, Eq. (30) cannot be used for the real part. However, replacing Eq. (30) by

$$\text{Re}A_{11}(s, t) = \tan(\rho) \text{Im}A_{11}(s, t)|_{Eq. (21)} \quad (31)$$

we obtain the same result, that the real part of the amplitude turns out to be too large. Actually, Eq. (31) assumes that the scattering amplitude depends on energy as a power $A(s, t) \propto s^{2\rho/\pi}$. Our amplitude is a rather complex function of energy, and depends on $\ln(s)$.

Variant of the fit	Δ_{dressed}	p_{01}	m_1 (GeV)	μ_1 (GeV)	ν_1	ν_2	κ_1
one channel model	0.48 ± 0.01	0.8 ± 0.05	0.860	7.6344	0.9	0.1	0.48

TABLE III: Fitted parameters for $d\sigma_{el}/dt$ dependence. $\Delta_{\text{dressed}} = \Delta(1 - p_{01})$.

Concluding, we see that to describe the TOTEM experimental data in the framework of our model, the contribution to the real part of the amplitude from the exchange of the odderon[28] is needed. Hence, our estimates confirm the

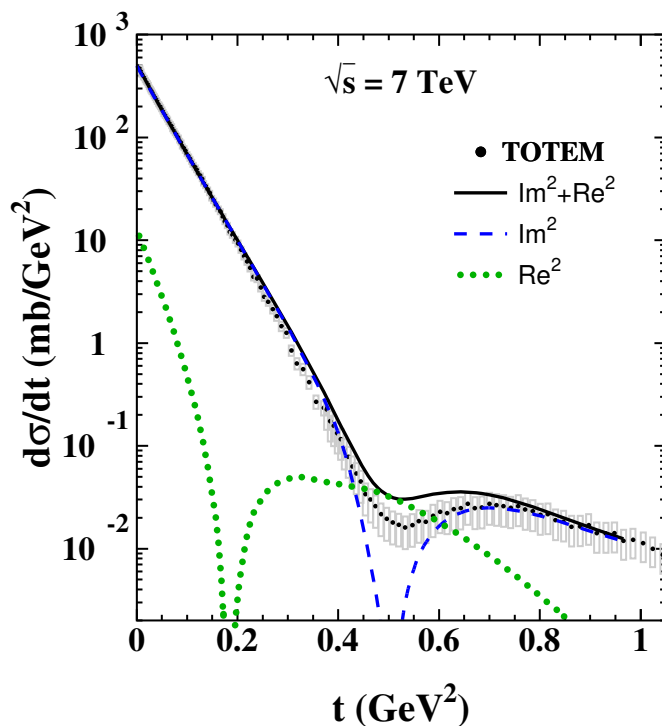


FIG. 7: $d\sigma_{el}/dt$ versus t . The solid line describes the result of our fit. The dotted line corresponds to the contribution of the real part of the scattering amplitude to the elastic cross section, which is calculated using Eq. (30), with added contribution of the exchange of the ω - reggeon, which is taken from Ref.[27]. We do not show the contribution of the real part without the ω -reggeon since it coincides with the dotted line. The dashed line is the contribution of the imaginary part of the amplitude. The data are taken from Ref.[26])

conclusions of Ref.[29]. In Fig. 6 we plot the description of the elastic cross section in which we add the odderon contribution to the amplitude of Eq. (21) (red solid curve in Fig. 6):

$$f(s, t) = f(s, t; Eq. (21)) \pm \sigma_{\text{odd}} e^{B_{\text{odd}} t} \quad (32)$$

where we consider a QCD odderon[28]: the state with odd signature and with the intercept $\alpha_{\text{odd}}(t=0) = 1$, which contributes only to the real part of the scattering amplitude. The value of $\sigma_{\text{odd}} = 20.6 \bar{\alpha}_S^3 mb \approx 0.5 mb$ for $\bar{\alpha}_S = 0.3$ in Eq. (32) we take from the QCD estimates in Ref.[30]. The value of $B_{\text{odd}} = 5.6 GeV^{-2}$ which is smaller than elastic slope for the BFKL Pomeron in accord with QCD estimates[30]. The sign minus in Eq. (32) corresponds to proton-proton scattering, while the sign plus stands for antiproton-proton collisions. Our odderon parameters are in accord with the estimates in Ref.[19]. The amplitude $f(s, t)$ is related to $a_{el}(s, b)$ by Eq. (25) (see also Eq. (22)).

In Fig. 8 we show the prediction for proton-antiproton scattering. One can conclude that in our model the measurements of the elastic cross sections for pp and $\bar{p}p$ scattering can provide the estimates for the odderon contribution. It should be stressed that the contribution of the ω -reggeon leads to negligible contribution at $W = 7 TeV$ (see Fig. 7).

CONCLUSIONS

In this paper we showed that the experimental data for proton-proton scattering at high energies can be described in the framework of the new parton model. The model is based on Pomeron calculus in 1+1 space-time, suggested in Ref. [4], and on the simple assumptions on the hadron structure, related to the impact parameter dependence of the scattering amplitude. This parton model stems from QCD, assuming that the unknown non-perturbative corrections lead to fixing the size of the interacting dipoles. The advantage of this approach is that it satisfies both t-channel and s-channel unitarity, and it can be used for summing all diagrams of the Pomeron interaction including the Pomeron

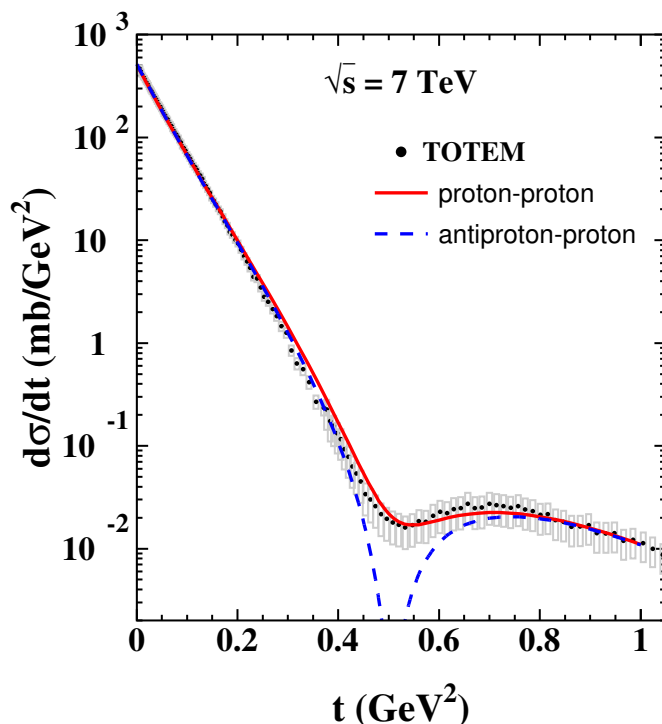


FIG. 8: $d\sigma_{el}/dt$ versus t . The solid line describes the elastic cross sections for pp -scattering with the odderon contribution (see Eq. (32)), while the dashed line shows the elastic cross section for $\bar{p}p$ -scattering using Eq. (32). The data are taken from Ref.[26])

loops. In other words, we can use this approach for all possible reactions: dilute-dilute (hadron-hadron), dilute-dense (hadron - nucleus) and dense-dense (nucleus-nucleus) parton system scattering. Unfortunately, we are far from solving this problem in the QCD effective theory at high energy (CGC /saturation approach).

We achieved a fairly good description of three experimental observables: $\sigma_{tot}, \sigma_{el}$ and B_{el} , especially as related to the energy dependence of these observables. We consider a success of the model, that we are able to describe the data on the single diffractive production in the two channel model.

The impact parameter dependance of the scattering amplitudes (see Fig. 4) shows that the soft interaction at high energies measured at the LHC have a much richer structure that we presumed in the past. We believe that we have demonstrated that the character of high energy scattering is closely related to the structure of hadron, which presently is described by a simple two channel model.

Our attempt to describe the t -dependence of the elastic cross section shows that we can reproduce the main features of the t -dependence that are measured experimentally: the slope of the elastic cross section at small t , the existence of the minima in t -dependence which is located at $|t|_{min} = 0.52 GeV^2$ at $W = 7 TeV$; and the behaviour of the cross section at $|t| > |t|_{min}$. It is still a challenge for us to find the theoretical description for the real part of the amplitude in the vicinity of t_{min} . In our model the real part turns out to be much smaller than the experimental one. Consequently, to achieve a description of the data, it is necessary to add an odderon contribution. Hence, our model corroborates the conclusion of Ref.[29].

A topic for future study, is whether the characteristic behaviour of the $A_{i,k}(b)$ amplitudes as a function of b stems from the theory of interacting Pomerons, which satisfies both s and t channel unitarity, or is an artifact of the simple two channel approach with the phenomenological input, on the impact parameter dependence.

We are aware that our model is very naive in describing the hadron structure, but hope that further progress in accumulating data on diffraction production, as well as the unsolved problem of treating the processes of the multiparticle generation in the framework of our approach, will generate a self consistent picture for high energy scattering at long distances.

Acknowledgements.

We thank our colleagues at Tel Aviv University and UTFSM for encouraging discussions. Our special thanks go to

Tamas Csörgő and Jan Kasper for discussion of the odderon contribution and elastic scattering during the Low x' 2019 WS. This research was supported by CONICYT PIA/BASAL FB0821(Chile) and Fondecyt (Chile) grants 1170319 and 1180118 .

* Electronic address: gotsman@post.tau.ac.il

† Electronic address: leving@tauex.tau.ac.il, eugenylevin@usm.cl

‡ Electronic address: irina.potashnikova@usm.cl

- [1] E. Gotsman, E. Levin and I. Potashnikova, “A new parton model for the soft interactions at high energies,” Eur. Phys. J. C **79** (2019) no.3, 192, [arXiv:1812.09040 [hep-ph]].
- [2] A. Kovner, E. Levin and M. Lublinsky, “QCD unitarity constraints on Reggeon Field Theory,” JHEP **1608** (2016) 031, [arXiv:1605.03251 [hep-ph]].
- [3] Y. V. Kovchegov and E. Levin *Quantum chromodynamics at high energy* Vol. 33 (Cambridge University Press, 2012).
- [4] T. Altinoluk, A. Kovner, E. Levin and M. Lublinsky, “Reggeon Field Theory for Large Pomeron Loops,” JHEP **1404** (2014) 075 [arXiv:1401.7431 [hep-ph]].
- [5] V. S. Fadin, E. A. Kuraev and L. N. Lipatov, “On the pomeranchuk singularity in asymptotically free theories”, Phys. Lett. **B60**, 50 (1975); E. A. Kuraev, L. N. Lipatov and V. S. Fadin, “The Pommeranchuk Singularity in Nonabelian Gauge Theories” Sov. Phys. JETP **45**, 199 (1977), [Zh. Eksp. Teor. Fiz.72,377(1977)]; I. I. Balitsky and L. N. Lipatov, “The Pommeranchuk Singularity in Quantum Chromodynamics,” Sov. J. Nucl. Phys. **28**, 822 (1978), [Yad. Fiz.28,1597(1978)].
- [6] E. Gotsman, E. Levin and I. Potashnikova, “CGC/saturation approach: soft interaction at the LHC energies,” Phys. Lett. B **781** (2018) 155, [arXiv:1712.06992 [hep-ph]].
- [7] E. Gotsman, E. Levin and I. Potashnikova, “A CGC/saturation approach for angular correlations in proton - proton scattering,” Eur. Phys. J. C **77** (2017) no.9, 632, [arXiv:1706.07617 [hep-ph]].
- [8] E. Gotsman, E. Levin and U. Maor, “A model for strong interactions at high energy based on the CGC/saturation approach,” Eur. Phys. J. C **75** (2015) 1, 18 [arXiv:1408.3811 [hep-ph]].
- [9] E. Gotsman, E. Levin and U. Maor, “CGC/saturation approach for soft interactions at high energy: a two channel model,” Eur. Phys. J. C **75** (2015) 5, 179 [arXiv:1502.05202 [hep-ph]].
- [10] E. Gotsman, E. Levin and U. Maor, “CGC/saturation approach for soft interactions at high energy: inclusive production,” Phys. Lett. B **746** (2015) 154 [arXiv:1503.04294 [hep-ph]].
- [11] E. Gotsman, E. Levin and U. Maor, “CGC/saturation approach for soft interactions at high energy: long range correlations,” Eur. Phys. J. C **75** (2015) 11, 518 [arXiv:1508.04236 [hep-ph]].
- [12] E. Gotsman, E. Levin and U. Maor, “CGC/saturation approach for soft interactions at high energy: survival probability of central exclusive production,” Eur. Phys. J. C **76** (2016) no.4, 177, [arXiv:1510.07249 [hep-ph]].
- [13] E. Gotsman, E. Levin, U. Maor and S. Tapia, “CGC/saturation approach for high energy soft interactions: v_2 in proton-proton collisions,” Phys. Rev. D **93** (2016) no.7, 074029, [arXiv:1603.02143 [hep-ph]].
- [14] M. A. Braun, “Nucleus-nucleus scattering in perturbative QCD with $N_c \rightarrow \infty$ Phys. Lett. B **483**, 115 (2000); e-Print Archive:[hep-ph/0003004]; “Nucleus nucleus interaction in the perturbative QCD,” Eur. Phys. J. C **33**, 113 (2004) e-Print Archive: [hep-ph/0309293]; “Conformal invariant pomeron interaction in the perturbative QCD with large N_c ,” Phys. Lett. B **632**, 297 (2006)
- [15] M. Froissart, “Asymptotic Behavior and Subtractions in the Mandelstam Representation”, Phys. Rev. **123** (1961) 1053; A. Martin, “Scattering Theory: Unitarity, Analyticity and Crossing.” Lecture Notes in Physics, Springer-Verlag, Berlin-Heidelberg-New-York, 1969.
- [16] I. Gradshteyn and I. Ryzhik, *Table of Integrals, Series, and Products*, Fifth Edition, Academic Press, London, 1994.
- [17] The Review of Particle Physics (2018), M. Tanabashi et al. (Particle Data Group), Phys. Rev. D **98**, 030001 (2018).
- [18] G. Antchev et al. [TOTEM Collaboration], “First measurement of elastic, inelastic and total cross-section at $\sqrt{s} = 13$ TeV by TOTEM and overview of cross-section data at LHC energies,” CERN-EP-2017-321, CERN-EP-2017-321-V2 arXiv:1712.06153 [hep-ex]; “First determination of the ρ parameter at $\sqrt{s} = 13$ TeV probing the existence of a colourless three-gluon bound state,” CERN-EP-2017-335, Submitted to: Phys.Rev..
- [19] V. A. Khoze, A. D. Martin and M. G. Ryskin, “Elastic and diffractive scattering at the LHC,” Phys. Lett. B **784**, 192 (2018) doi:10.1016/j.physletb.2018.07.054 [arXiv:1806.05970 [hep-ph]].
- [20] M. L. Good and W. D. Walker, “Diffraction Dissociation of Beam Particles”, Phys. Rev. **120** (1960) 1857.
- [21] G. Gustafson, “The Relation between the Good-Walker and Triple-Regge Formalisms for Diffractive Excitation,” Phys. Lett. B **718** (2013) 1054, [arXiv:1206.1733 [hep-ph]].
- [22] Jan Kasper, “Soft diffraction at LHC”, EPJ Web of Conference **72**, 06005(2018), <https://doi.org/10.105/epjconf/2018172060005>.
- [23] A. B. Kaidalov and M. G. Poghosyan, “Predictions of Quark-Gluon String Model for pp at LHC,” Eur. Phys. J. C **67** (2010) 397 doi:10.1140/epjc/s10052-010-1301-y [arXiv:0910.2050 [hep-ph]]; “Description of soft diffraction in the framework of reggeon calculus: Predictions for LHC,” arXiv:0909.5156 [hep-ph], talk given at 13th International Conference on Elastic and Diffractive Scattering (Blois Workshop): “Moving Forward into the LHC Era (EDS 09) .
- [24] V. P. Gonsalves, R. P. da Silva and P. V. R. G. Silva, “Diffractive excitation in pp and pA collisions at high energies,” Phys. Rev. D **100** (2019) no.1, 014019 doi:10.1103/PhysRevD.100.014019 [arXiv:1905.00806 [hep-ph]].

- [25] H. I. Miettinen and J. Pumplin, “*Diffraction Scattering and the Parton Structure of Hadrons*,” Phys. Rev. D **18** (1978) 1696. doi:10.1103/PhysRevD.18.1696
- [26] G. Antchev *et al.* [TOTEM Collaboration], “*Measurement of proton-proton elastic scattering and total cross-section at $\sqrt{s} = 7\text{-TeV}$* ,” EPL **101** (2013) no.2, 21002. doi:10.1209/0295-5075/101/21002
- [27] A. Donnachie and P. V. Landshoff, “*pp and $\bar{p}p$ total cross sections and elastic scattering*,” Phys. Lett. B **727** (2013) 500 Erratum: [Phys. Lett. B **750** (2015) 669] doi:10.1016/j.physletb.2015.09.017, 10.1016/j.physletb.2013.10.068 [arXiv:1309.1292 [hep-ph]].
- [28] J. Bartels, L. N. Lipatov and G. P. Vacca, “*A New odderon solution in perturbative QCD*,” Phys. Lett. B **477** (2000) 178 doi:10.1016/S0370-2693(00)00221-5 [hep-ph/9912423]; Y. V. Kovchegov, L. Szymanowski and S. Wallon, “*Perturbative odderon in the dipole model*,” Phys. Lett. B **586** (2004) 267 doi:10.1016/j.physletb.2004.02.036 [hep-ph/0309281].
- [29] T. Csörgő, T. Novak, R. Pasechnik, A. Ster and I. Szanyi, “*Evidence of Odderon-exchange from scaling properties of elastic scattering at TeV energies*,” arXiv:1912.11968 [hep-ph].
- [30] M. G. Ryskin, “*Odderon and Polarization Phenomena in QCD*,” Sov. J. Nucl. Phys. **46** (1987) 337 [Yad. Fiz. **46** (1987) 611]; E. M. Levin and M. G. Ryskin, “*High-energy hadron collisions in QCD*,” Phys. Rept. **189** (1990) 267.